HCF-1 Amino- and Carboxy-Terminal Subunit Association through Two Separate Sets of Interaction Modules: Involvement of Fibronectin Type 3 Repeats

Angus C. Wilson, Michael Boutros, Kristina M. Johnson and Winship Herr

Updated information and services can be found at:
http://mcb.asm.org/content/20/18/6721

These include:

REFERENCES
This article cites 28 articles, 16 of which can be accessed free
at: http://mcb.asm.org/content/20/18/6721#ref-list-1

CONTENT ALERTS
Receive: RSS Feeds, eTOCs, free email alerts (when new
articles cite this article), more»

HCF-1 Amino- and Carboxy-Terminal Subunit Association through Two Separate Sets of Interaction Modules: Involvement of Fibronectin Type 3 Repeats

ANGUS C. WILSON,[1,2] MICHAEL BOUTROS,[1]† KRISTINA M. JOHNSON,[2]‡ AND WINSHIP HERR[1]*

Cold Spring Harbor Laboratory, Cold Spring Harbor, New York 11724,[1] and Department of Microbiology and Kaplan Cancer Center, New York University School of Medicine, New York, New York 10016[2]

When herpes simplex virus infects permissive cells, the viral regulatory protein VP16 forms a specific complex with HCF-1, a preexisting nuclear protein involved in cell proliferation. The majority of HCF-1 in the cell is a complex of associated amino (HCF-1$_N$)- and carboxy (HCF-1$_C$)-terminal subunits that result from an unusual proteolytic processing of a large precursor polypeptide. Here, we have characterized the structure and function of sequences required for HCF-1$_N$ and HCF-1$_C$ subunit association. HCF-1 contains two matched pairs of self-association sequences called SAS1 and SAS2. One of these matched association sequences, SAS1, consists of a short 43-amino-acid region of the HCF-1$_N$ subunit, which associates with a carboxy-terminal region of the HCF-1$_C$ subunit that is composed of a tandem pair of fibronectin type 3 repeats, a structural motif known to promote protein-protein interactions. Unexpectedly, the related protein HCF-2, which is not proteolyzed, also contains a functional SAS1 association element, suggesting that this element does not function solely to maintain HCF-1$_N$ and HCF-1$_C$ subunit association. HCF-1$_N$ subunits do not possess a nuclear localization signal. We show that, owing to a carboxy-terminal HCF-1 nuclear localization signal, HCF-1$_C$ subunits can recruit HCF-1$_N$ subunits to the nucleus.

Lytic infection of human cells by herpes simplex virus is characterized by a cascade of viral gene expression initiated by the virion protein VP16 (reviewed in reference 22). Following infection of the host cell, the viral transactivator VP16 (also known as Vmw65 and αTIF) is released from the virion, whereupon it associates with two preexisting nuclear factors, Oct-1 and HCF-1, to form a multiprotein-DNA complex on VP16-responsive *cis*-regulatory elements in the viral immediate-early promoters (8).

Oct-1 is a broadly expressed POU homeodomain-containing transcription factor (24). The function of HCF-1 (also known as HCF, C1, VCAF, and CFF) in the uninfected cell is less well understood. The principal HCF-1 translation product is a large protein of 2,035 amino acids (12, 27), but only an amino-terminal region of about 380 amino acids is essential for HCF-1 interaction with VP16 and stabilization of the VP16-induced complex with Oct-1 (10, 15, 26). Characterization of a temperature-sensitive hamster cell line called tsBN67 has indicated that HCF-1 is involved in cell proliferation (7): at nonpermissive temperature, tsBN67 cells stop proliferating owing to a missense mutation within the HCF-1 VP16 interaction region, which also inhibits HCF-1 association with VP16 (7, 26). The molecular mechanisms, however, by which HCF-1 regulates cell proliferation are not known.

HCF-1 is a member of a protein family that includes the recently described human protein HCF-2 (11), and both HCF-1 and HCF-2 are related to a protein in the worm *Caenorhabditis elegans* called CeHCF (16). These three proteins have conserved the VP16 interaction region and associate with VP16 to differing extents (11, 16).

In mammalian cells, HCF-1 undergoes an unusual maturation process. Its primary translation product is cleaved at a series of six conserved 26-amino-acid repeats called HCF$_{PRO}$ repeats located near the center of the primary translation product (12, 27, 29). The resulting fragments, called HCF-1$_N$ and HCF-1$_C$, are stable, and they remain noncovalently associated, creating a mature HCF-1 complex (29). Although the majority of HCF-1$_N$ and HCF-1$_C$ subunits remain noncovalently associated after proteolysis, there is a variant HCF-1 translation product called HCF-1$_{\Delta382-450}$, which results from removal of an exon encoding amino-terminal HCF-1 residues 382 to 450 through alternative pre-mRNA processing; this smaller HCF-1 protein undergoes proteolytic processing, but the resulting HCF-1$_N$ and HCF-1$_C$ subunits do not remain associated (29). Unlike the HCF-1 protein, HCF-2 and CeHCF do not possess HCF$_{PRO}$ repeats, and HCF-2 is not proteolytically cleaved like HCF-1 (11).

HCF-1 processing and the subsequent association of the resulting HCF-1$_N$ and HCF-1$_C$ subunits are unusual, and little is known concerning the mechanisms by which they occur. Here, we describe aspects of human HCF-1$_N$ and HCF-1$_C$ subunit association. Our results show that the HCF-1$_N$ and HCF-1$_C$ subunits contain two matched pairs of subunit association elements and that subunit association can permit recruitment of HCF-1$_N$ subunits to the nucleus via a nuclear localization signal (NLS) located at the carboxyl terminus of the HCF-1$_C$ subunit. Unexpectedly, HCF-2, which is not proteolyzed, shares one of the HCF-1 subunit association elements, suggesting that the role of such an element is not solely to maintain HCF-1$_N$ and HCF-1$_C$ subunit association.

* Corresponding author. Mailing address: Cold Spring Harbor Laboratory, P.O. Box 100, Cold Spring Harbor, NY 11724. Phone: (516) 367-8401. Fax: (516) 367-8454. E-mail: herr@cshl.org.

† Present address: Department of Genetics, Harvard Medical School, Boston, MA 02115.

‡ Present address: Department of Biological Chemistry, University of California, Los Angeles, School of Medicine, Los Angeles, CA 90095.

MATERIALS AND METHODS

Mammalian expression plasmids. The hemagglutinin (HA)-epitope-tagged human HCF expression constructs pCGNHCF$_{N1011\Delta382-450}$, pCGNHCF$_{N450-1011}$, pCGNHCF$_{N450}$, and pCGNHCF$_{N380}$ have been described previously (26). pCGTHCF$_C$ (C-terminal residues 1436 to 2035) is identical to pCGNHCF$_C$ (26) except that the influenza virus HA epitope is replaced by a bacteriophage T7 gene 10 (T7) epitope. To ensure detection and protein stability, HCF-1 residues 348 to 450 or smaller derivatives were expressed as fusions to the GAL4 DNA-binding domain (residues 1 to 94) by subcloning into pCGNGAL4(1–94). pCGTHCF$_{SAS2C}$ encodes HCF-1 residues 1436 to 1756, and pCGTHCF$_{SAS1C}$ encodes residues 1758 to 2035. Truncations were generated either by using suitable restriction sites or by PCR or oligonucleotide-mediated mutagenesis. A fragment spanning residues 341 to 394 of human HCF-2 (11) was amplified using PCR and subcloned into pCGNGAL4(1–94). The nucleotide sequences of PCR-generated fragments were verified by DNA sequencing.

Sequence analysis. Searches of the protein databases were performed using BLASTP (1) and SMART (Simple Modular Architecture Research Tool) (23). Sequence alignments were compiled using ZEGA and CLUSTALW (provided on-line by the Molecular Modeling and Bioinformatics Group, Skirball Institute, New York University School of Medicine).

Transfections, immunoprecipitations, and immunoblotting. Human 293 and 293T cells were transfected by electroporation or with Lipofectamine (Gibco BRL, Inc.), respectively (11, 26). Preparation of whole-cell nuclear extracts, immunoprecipitation, and immunoblotting were performed as described previously (26).

Immunofluorescence. 293 cells were transfected by electroporation and seeded onto sterile coverslips. After 36 h, the coverslips were washed in phosphate-buffered saline (PBS); the cells were fixed in 4% paraformaldehyde for 20 min and permeabilized for 5 min with PBS containing 0.1% Triton X-100. The samples were then washed three times with PBS and blocked for 30 min in PBS containing 2% dry milk. After washing in PBS, coverslips were incubated for 45 min with the primary antibody, washed, and incubated with the secondary antibody for an additional 45 min. Fluorescence was observed with a Nikon fluorescence microscope or a Zeiss confocal microscope.

RESULTS

Figure 1A shows a schematic of the structure of the primary human HCF-1 translation product called HCF-1$_{300}$. HCF-1$_{300}$ contains two previously described sets of repeat elements: centrally located HCF-1$_{PRO}$ repeats and six amino-terminal kelch-like repeats called HCF-1$_{KEL}$, which likely fold into a six-bladed β-propeller structure (residues 17 to 360 [15, 26]). Here, we analyzed the sequence of the carboxy-terminal region of HCF-1, which was originally described as rich in charged residues and the large hydrophobic residues tryptophan, tyrosine, and phenylalanine (27). This region has been conserved in evolution: both HCF-2 (11) and CeHCF (16) share extensive sequence similarity to residues 1812 to 2001 of HCF-1 (Fig. 1B). This region also exhibits internal sequence similarity, which indicates a repeat of HCF-1 residues 1812 to 1875 and 1910 to 1992. These two sequences share a conserved tryptophan (W) residue (positions 1812 and 1910) and the interdigitated sequence FRXXXXNXXGXG, where "X" indicates any amino acid (residues 1864 to 1875 and 1981 to 1992 [Fig. 1B]).

A comparison of each carboxy-terminal repeat with other protein sequences using the BLASTP program (1) and also the SMART database (23) revealed significant similarity to fibronectin type 3 (Fn3) repeats. Fn3 repeats are typically 90 to 100 residues long and, although exhibiting relatively low primary amino acid sequence similarity among different proteins, display considerable structural similarity (reviewed in reference 2). Figure 1C shows a sequence alignment of four Fn3 repeats from the β$_4$ subunit of α$_6$β$_4$ integrin. The first two (Fn3-1 and Fn3-2) and second two (Fn3-3 and Fn3-4) represent tandem repeats as with the two repeats in HCF-1. The structure of the first set of tandem repeats has been determined (3), and the positions of β strands in the structure are shown in Fig. 1C. Together, Fig. 1B and C show the similarity of the two carboxy-terminal HCF-1 repeats to Fn3 repeats. The predicted Fn3 repeats in HCF-1 have also been identified independently by the SMART database (http://smart.embl-heidelberg.de).

These sequence analyses identify for the first time a predicted structural element within the carboxy-terminal region of HCF-1. We therefore refer to these carboxy-terminal HCF-1 repeats as HCF-1$_{Fn3}$1 and HCF-1$_{Fn3}$2.

The HCF-1$_N$ and HCF-1$_C$ subunits readily associate when synthesized separately. In the mature endogenous HCF-1 complex, the noncovalently associated HCF-1$_N$ and HCF-1$_C$ subunits result from proteolytic processing of the HCF-1$_{300}$ precursor (29); thus, the HCF-1$_N$ and HCF-1$_C$ subunits are in close proximity for coassociation prior to proteolytic cleavage. HCF-1$_N$ and HCF-1$_C$ subunit association might, however, be regulated through sequential dissociation and reassociation. To test the feasibility of such a hypothesis, we asked whether dissociated HCF-1$_N$ and HCF-1$_C$ subunits can associate without prior tethering as a single translation product.

We cotransfected human 293 cells with plasmids separately encoding engineered HCF-1$_N$ (HCF-1$_{N1011}$) and HCF-1$_C$ (HCF-1$_{C600}$) subunits. The HCF-1$_N$ subunit was tagged at its amino terminus with an influenza virus HA epitope, and the HCF-1$_C$ subunit was tagged at its amino terminus with a T7 epitope. As a positive control for protein-protein association, we coexpressed the HCF-1$_N$ subunit with a T7-tagged VP16 protein (26). Protein extracts were prepared from the transfected cells, and the HA-tagged amino-terminal polypeptide was recovered by immunoprecipitation with an anti-HA (αHA) monoclonal antibody. The resulting immune complexes were resolved on a sodium dodecyl sulfate (SDS)-polyacrylamide gel, and the coimmunoprecipitated HCF-1$_C$ and VP16 proteins were detected by immunoblotting with an αT7 monoclonal antibody.

Figure 2 shows the result of such an experiment. Neither VP16 nor the HCF-1$_C$ subunit was recovered in the absence of HA-HCF-1$_N$ subunit expression (lanes 2 and 3), but both were recovered effectively in the presence of the full-length HCF-1$_N$ subunit HA-HCF-1$_{N1011}$ (compare lanes 4 and 5). This result demonstrates that HCF-1$_N$ and HCF-1$_C$ subunit association is not dependent on coexpression as the HCF-1$_{300}$ precursor and indicates that the association of HCF-1$_N$ and HCF-1$_C$ subunits in endogenous HCF-1 can be dynamic.

The HCF-1$_N$ subunit contains two HCF-1$_C$ subunit association regions. We have previously shown that the natural HCF-1 variant HCF-1$_{\Delta382-450}$ (Fig. 1A) is processed normally, but the resulting HCF$_{N\Delta382-450}$ and HCF$_C$ subunits do not remain associated (29). Consistent with this observation, when synthesized separately as shown in Fig. 2, an HCF-1$_N$ subunit lacking residues 382 to 450 but retaining the VP16 interaction region (HCF-1$_{N1011\Delta382-450}$) bound VP16 (lane 6) but not the engineered HCF-1$_C$ subunit (lane 7), suggesting that loss of residues 382 to 450 disrupts sequences involved in HCF-1$_N$ association with the HCF-1$_C$ subunit.

To map more precisely the HCF-1$_N$ region(s) involved in HCF-1 subunit association, we divided the HCF-1$_N$ subunit into two segments, with one fragment containing residues 1 to 450 (HCF-1$_{N450}$)—thus including the 382–450 region involved in controlling HCF-1$_C$ subunit association—and the other spanning the remainder of the HCF-1$_N$ subunit (HCF-1$_{N450-1011}$). Consistent with previous studies (26), the HCF-1$_{N450}$ protein (Fig. 2, lane 8) but not the HCF-1$_{N450-1011}$ protein (lane 10) associated with VP16. To our surprise, however, both nonoverlapping HCF-1$_N$ derivatives associated with the HCF-1$_C$ subunit (lanes 9 and 11), suggesting that the HCF-1$_N$ subunit contains two HCF-1$_C$ association sequences. We refer to the regions involved in HCF-1$_N$ and HCF-1$_C$ subunit association as self-association sequence (SAS) elements; the SAS elements in HCF-1$_{N450}$ and HCF-1$_{N450-1011}$ are referred to as HCF-1$_{SAS1N}$ and HCF-1$_{SAS2N}$, respectively.

A

hHCF-1

- VP16 interaction
- HCF-1KEL Repeats
- HCF-1 Processing
- Δ382–450
- Basic
- 1 2 3 4　　5 6 7 8
- HCF-1PRO Repeats
- Acidic
- WYF Charged
- 1800　　1900　　2000 2015　　2035
- HCF-1Fn31　　HCF-1Fn32
- NLS

B

```
             A→                       B→
HCF-1  1800  PPSKAPMKRENQFDVGVIKGTNVMMTHYFLPP-DDAVPSDDDLGTVPDYNQLK
HCF-2   586  NPVATVKAGERQCDVGIFKNNTALVSQFYLLPKGKQSISKVGNADVPDYSLLK
CeHCF   541  EMKEENGDDDLPDFDVGIIDKATIVUTHYF---NDRQQSLEKQLNDLIDINAFK

             C→                  C'→                E→
HCF-1  ----SGKIIEYSVTLAIQSSQAGGELKSSTPAQIAFMRVYCGPSPSCLVQSSSLSNAHIDYTTKPAII   1897
HCF-2  ----SGNTLEYSAYTAIRTAQI----QDNPSQLVFMRIYCGLKTSCIVTAGQLANAHIDYTSRPAIV   684
CeHCF  ----IHEYSVTLAVKNQSA-----NSADSQLAFMRVYCGPQADCQVLQSNLGTAFVDQINKPAI       647

Invariant Residues                                                        W
```

```
             F→                               FR   N   G        G1→                      G2→
HCF-1  1898  FIAARNEKIYGPATQVRWI.QETSKDSSGTK...  KQELQPGTAFKFRVAGINACGPHFSEISAFKTCLPGFPGAPCAI   2011
HCF-2   685  FRISAKEKIYGPATQVRWI.QNNKKAAPLN*     KQDLVPGTGVFFRVAAINGCGIGFFSKISEFKTCIPGFPGAPSAV   792
CeHCF   648  FVDQINKPAI...                       KIPLINGQSYRFFVSAINGLGKGAWSETASCKTCVPGYPGAPSSI   758

Invariant Residues                          FR   N   G   G
```

C

```
           A→                  B→                  C→              C'→            E→
1131  QNPNAKAAGSRKIHFNWLPP---SGRKPMGYRVKVWIQGDS--ESEAHLLDSK---VPSVEL
1224  GRLAFNVVSSTVTQLSAEPAETNGEITAYEVCVGLVNDDNRPIGPMKKVLVDNPKNRMLLI
1462  TRLVFSALGPTSLRVSQEP-RCERPLQGYSVEVQYLLNGG---ELHRLNIP--NPAQTSVVV
1775  GPLVFTALSPDSLQLSWERPRRPNGDIVGYLVTCEMAQGG--GPATAFRVDGDSPESR-LTV

           F→                       G1→              G2→
1131  ------------TNLYPYCDYEMRVCAVCAQGEGPYSSLVSCRTHQE       β4 Fn3-1   1224
1224  ------ENLRESQPYVRTVKARNGACWGPE-REAIINLATQ             β4 Fn3-2   1462
1462  -----EDLLPNHSYVFRVRAQSPEGWGRE-REGVTIIESQ             β4 Fn3-3   1775
1775  ----------PGLSENVPYKFKVQARTEQGFGPE-REGITTIESQ         β4 Fn3-4
```
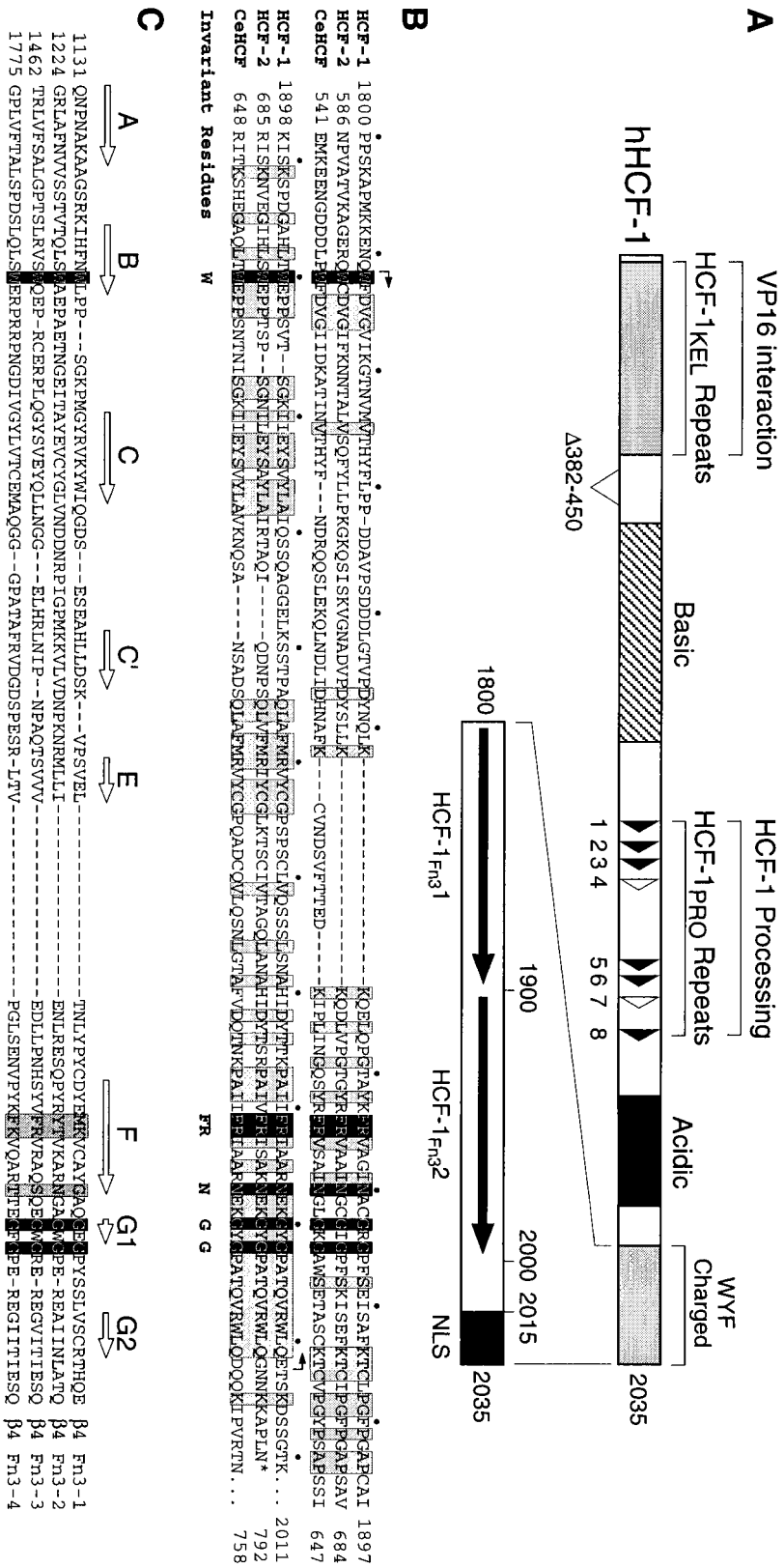
FIG. 1. HCF-1 contains two Fn3-like repeats. (A) Structural features of human HCF-1 (hHCF-1). The six near-perfect HCF-1$_{PRO}$ repeats (filled arrowheads) and two degenerate nonfunctional repeats (open arrowheads) are indicated. The amino-terminal β-propeller domain involved in association with VP16 is represented as a shaded box. A carboxy-terminal domain rich in charged or bulky hydrophobic residues (tryptophan, tyrosine, and phenylalanine) is shown in greater detail. This region contains two putative Fn3 repeats (HCF-1$_{Fn3}$1 and HCF-1$_{Fn3}$2), indicated by filled arrows. A bipartite NLS (filled box) lies at the very carboxyl terminus (13). Regions with overall basic or acidic charge are also indicated. The region Δ382–450 is deleted in a natural form of HCF-1 that results from alternative splicing of the HCF-1 transcript. (B) Alignment of the tandem HCF-1$_{Fn3}$1 and HCF-1$_{Fn3}$2 repeats from the carboxy termini of HCF-1, HCF-2, and CeHCF. The six perfectly conserved positions (invariant residues) are highlighted in black, while residues that are identical in each of the three HCF repeats are shaded. Small arrows denote the limits of the HCF-1$_{basic}$ element; dots over the HCF-1 sequence indicate 10-amino-acid segments. (C) Alignment of the four Fn3 repeats from the intracellular domain of integrin β4. The positions of β strands A through G2 (open arrows) are derived from the crystal structure of the tandem Fn3-1 and Fn3-2 modules from integrin α6β4 (3). In close agreement with other Fn3 structures, β strands A, B, and E and β strands C, C', F, G1, and G2 form two β sheets that pack as a β sandwich, enclosing a hydrophobic core (2). The invariant residues identified in HCF$_{Fn3}$1 and HCF$_{Fn3}$2 (shown below the sequences) are to a large extent conserved in all four modules of integrin β4.
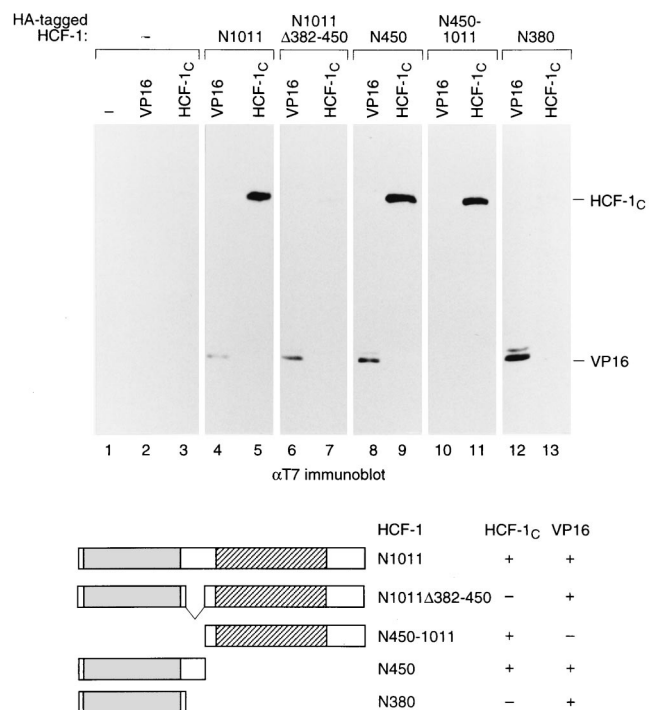
FIG. 2. HCF-1 contains two N-terminal domains that can mediate association with the C terminus. Extracts were prepared from 293 cells transfected with 5 μg of expression plasmids encoding HA-tagged derivatives of the HCF-1$_N$ subunit and with 2 μg of expression plasmids encoding a T7 epitope-tagged version of either VP16ΔC (VP16) or the HCF-1$_C$ subunit. HA-tagged polypeptides were recovered by immunoprecipitation with an αHA monoclonal antibody, resolved on an SDS–8% polyacrylamide gel, and immunoblotted with an αT7 tag antibody (Novagen) to detect coimmunoprecipitated VP16 or HCF-1$_C$ protein. The HA-tagged polypeptides were as follows: mock (lanes 1 to 3), HCF-1$_{N1011}$ (lanes 4 and 5), HCF-1$_{N1011Δ382-450}$ (lanes 6 and 7), HCF-1$_{N450}$ (lanes 8 and 9), HCF-1$_{N450-1011}$ (lanes 10 and 11), and HCF-1$_{N380}$ (lanes 12 and 13). The structures of HCF-1$_N$ and its derivatives used for coimmunoprecipitation are shown schematically below. The ability (+) or inability (−) of each amino-terminal fragment to interact with VP16 or HCF-1$_C$ is indicated.

The presence of an HCF-1$_N$ SAS element in the HCF-1$_{N450-1011}$ fragment was unexpected because the natural HCF-1$_{NΔ382-450}$ subunit encompasses all but one residue of the HCF-1$_{N450-1011}$ fragment and yet fails to associate with the HCF-1$_C$ subunit (Fig. 2, lane 7). Thus, loss of residues 382 to 450 in the HCF-1$_N$ subunit appears to have a dominant negative effect on the activity of HCF-1$_{SAS2N}$ element in HCF-1$_{N450-1011}$. Given this unexpected result, we asked whether the HCF-1$_{SAS1N}$ element in the HCF-1$_{N450}$ fragment (lane 9) might reside within the residues 1 to 380 (i.e., the VP16 interaction region), and its activity also be inhibited in the HCF-1$_{NΔ382-450}$ deletion variant, by assaying the ability of an HCF-1$_{N380}$ fragment to associate with the HCF-1$_C$ subunit. Consistent with previous results (26), the HCF-1$_{N380}$ fragment associated with VP16 (lane 12); it failed, however, to associate with the HCF-1$_C$ subunit (lane 13). Thus, the HCF-1$_{SAS1N}$ element does not reside entirely within the VP16-interaction region, and VP16 and HCF-1$_C$ subunit associations are different HCF-1$_N$ activities.

The HCF-1$_C$ subunit contains two independent HCF-1$_N$ association elements. Given the identification of two regions within the HCF-1$_N$ subunit that can associate independently with the HCF-1$_C$ subunit, HCF-1$_{SAS1N}$ and HCF-1$_{SAS2N}$, we asked whether these regions might associate with the same region or different regions of the HCF-1$_C$ subunit. In addition

to the Fn3 repeats, the HCF-1$_C$ subunit contains a region with more acidic than basic residues (reference 37 and Fig. 1A). To determine whether either the acidic or Fn3 repeat regions are involved in HCF-1$_N$ subunit association, we divided the HCF-1$_C$ subunit in two—residues 1436 to 1756 covering the acidic region (HCF-1$_{C1436-1756}$) and residues 1758 to 2035 covering the HCF-1$_{Fn3}$ repeats (HCF-1$_{C1758-2035}$)—and tested each individually for association with the HCF-1$_N$ subunit as shown in Fig. 3. In addition to associating with the full-length HCF-1$_C$ subunit (lane 1) as expected, the full-length HCF-1$_N$ subunit associated with both the acidic HCF-1$_{C1436-1756}$ (lane 2) and Fn3 repeat-containing HCF-1$_{C1758-2035}$ (lane 3) fragments, although recovery of the HCF-1$_{C1436-1756}$ fragment was considerably less efficient, which may reflect inhibition by the amino-terminal region of HCF-1 (see Discussion). In contrast, the alternative-splice variant HCF-1$_{NΔ382-450}$ subunit associates neither with the full-length HCF-1$_C$ subunit (lane 4), as expected, nor with either HCF-1$_C$ subfragment (lanes 5 and 6) effectively. Thus, the full-length but not the splice-variant HCF-1 can associate with two independent regions within the carboxy-terminal HCF-1$_C$ subunit. We refer to the most carboxy-terminal HCF-1$_C$ self-association sequence in the HCF-1$_{C1758-2035}$ segment as HCF-1$_{SAS1C}$ and the more internal HCF-1$_C$ self-association sequence in the HCF-1$_{C1436-1756}$ segment as HCF-1$_{SAS2C}$.

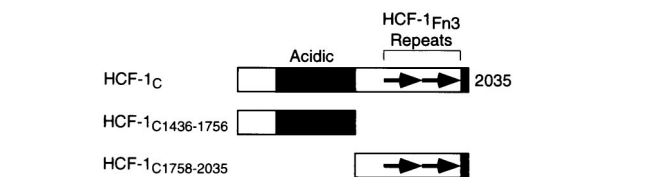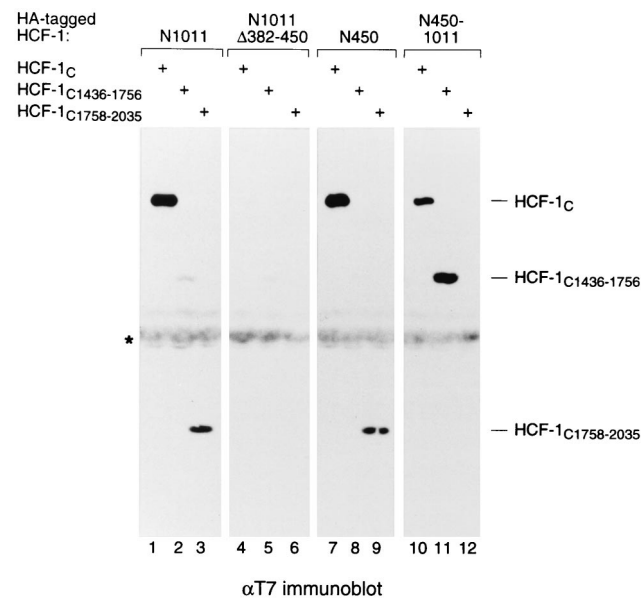Having identified two SAS elements in both the HCF$_N$ and

FIG. 3. HCF-1$_{SAS1N}$ and HCF-1$_{SAS2N}$ interact with different regions of the HCF$_C$ subunit. HA-tagged HCF-1$_N$ fragments and T7-tagged HCF$_C$ fragments were coexpressed in transfected 293 cells, and association was assayed by immunoprecipitation with the αHCF-1 antibody followed by immunoblotting with the αT7 antibody. The HA-tagged polypeptides were as follows: HCF-1$_{N1011}$ (lanes 1 to 3), HCF-1$_{N1011Δ382-450}$ (lanes 4 to 6), HCF-1$_{N450}$ (lanes 7 to 9), and HCF-1$_{N450-1011}$ (lanes 10 to 12). The T7-tagged polypeptides were as follows: HCF-1$_C$ (lanes 1, 4, 7, and 10), HCF-1$_{C1436-1756}$ (lanes 2, 5, 8, and 11), and HCF-1$_{C1758-2035}$ (lanes 3, 6, 9, and 12).
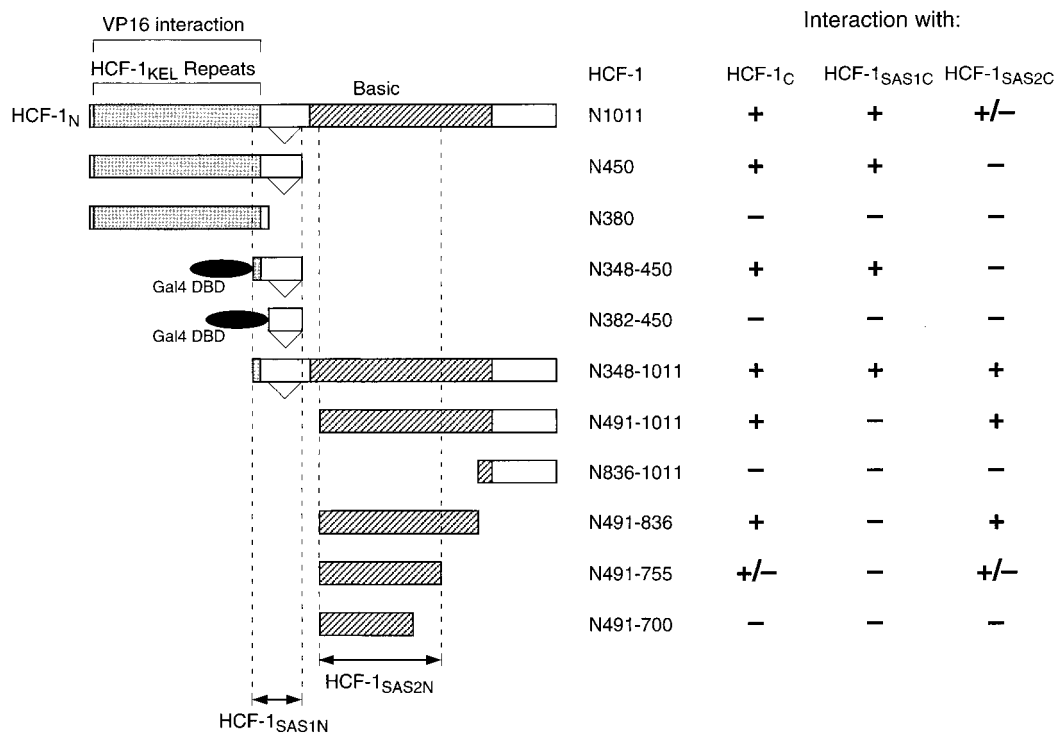
HCF-1	HCF-1$_C$	HCF-1$_{SAS1C}$	HCF-1$_{SAS2C}$
N1011	+	+	+/−
N450	+	+	−
N380	−	−	−
N348-450	+	+	−
N382-450	−	−	−
N348-1011	+	+	+
N491-1011	+	−	+
N836-1011	−	−	−
N491-836	+	−	+
N491-755	+/−	−	+/−
N491-700	−	−	−

FIG. 4. Summary of mapping of the HCF-1$_N$ SAS elements. Each HCF-1$_N$ derivative was assayed for association with HCF-1$_C$ (residues 1436 to 2035), HCF-1$_{SAS1C}$ (residues 1758 to 2035), and HCF-1$_{SAS2C}$ (residues 1436 to 1756) by coimmunoprecipitation from transfected 293 cell extracts. The interactions were scored as strong (+), weak (+/−), or not detected (−). HCF-1$_{N348–450}$ and HCF-1$_{N382–450}$ were unstable as isolated polypeptides and were assayed as fusions to the GAL4 DNA-binding domain (residues 1 to 94).

HCF$_C$ subunits, we asked whether there is any specificity in the interaction between the amino-terminal HCF-1$_{SAS1N}$ and HCF-1$_{SAS2N}$ elements and the carboxy-terminal HCF-1$_{SAS1C}$ and HCF-1$_{SAS2C}$ elements as shown in Fig. 3. Indeed, there is specificity: the HCF-1$_{SAS1N}$-containing HCF-1$_{N450}$ fragment associated only with the HCF-1$_{SAS1C}$-containing HCF-1$_{C1758–2035}$ fragment (compare lanes 7 to 9), and the HCF-1$_{SAS2N}$-containing HCF-1$_{N450–1011}$ fragment associated only with the HCF-1$_{SAS2C}$-containing HCF-1$_{C1436–1756}$ fragment (compare lanes 10 to 12). Thus, HCF-1 displays two matched pairs of SAS elements: the most amino- and carboxy-terminal SAS elements—HCF-1$_{SAS1N}$ and HCF-1$_{SAS1C}$—form one association complex, and the more internal SAS elements—HCF-1$_{SAS2N}$ and HCF-1$_{SAS2C}$—form a second association complex. We do not know, however, whether both SAS1 and SAS2 mediate HCF-1$_N$ and HCF-1$_C$ subunit association simultaneously in native HCF-1.

Mapping of the amino-terminal HCF-1$_{SAS1N}$ and HCF-1$_{SAS2N}$ elements. Using the strategy shown in Fig. 3, in experiments not shown here we refined the location of the HCF-1$_{SAS1N}$ and HCF-1$_{SAS2N}$ elements. The results of these experiments are summarized in Fig. 4. As shown in Fig. 3, HCF-1$_{N1011}$ associated with both HCF-1$_{SAS1C}$ and to a lesser extent with HCF-1$_{SAS2C}$, whereas HCF-1$_{N450}$ associated effectively only with the HCF-1$_{SAS1C}$ element. Consistent with the inability of the minimal VP16 interaction region in HCF-1$_{N380}$ to associate with the entire HCF-1$_C$ subunit (Fig. 2), HCF-1$_{N380}$ did not exhibit association with either the HCF-1$_{SAS1C}$ or HCF-1$_{SAS2C}$ element. In these experiments, we mapped the HCF-1$_{SAS1N}$ element to within HCF residues 348 to 450 (which we fused to the yeast GAL4 DNA-binding domain owing to our inability to detect this and smaller HCF fragments of this region on their own in our assay). Residues 382 to 450

alone, however, which represent the region removed in the alternative-splice variant of HCF, failed to associate with any of the HCF-1$_C$ fragments (Fig. 4). Consistent with this mapping of the HCF-1$_{SAS1N}$ element, a fragment covering residues 348 to 1011 (HCF-1$_{N348–1011}$) associated with all three of the HCF-1$_C$ fragments used in the coimmunoprecipitation assay.

Analysis of a selection of fragments containing portions of a region enriched in basic residues (Fig. 1A)—HCF-1$_{N491–1011}$, HCF-1$_{N836–1011}$, HCF-1$_{N491–836}$, HCF-1$_{N491–755}$, and HCF-1$_{N491–700}$—narrows the location of the HCF-1$_{SAS2N}$ element to within HCF residues 491 to 755 (Fig. 4). These results show that a subregion of the basic region contains the HCF-1$_{SAS2N}$ element. Residues 813 to 847 within the basic region have recently been shown to associate with the transcription factor GA-binding protein (GABP) (25). This association is unlikely to be related to the SAS2N function because these two elements of HCF-1 do not overlap each other (residues 491 to 755 [SAS2N] versus 813 to 847 [GABP association]).

The basic region has previously been implicated in cell proliferation, and HCF-1$_N$ sequences extending past residue 836 but not beyond residue 902 are required to rescue the temperature-sensitive defect in the hamster tsBN67 cell line (26). The ability of the HCF-1$_{N491–836}$ fragment to associate effectively with the HCF-1$_{SAS2C}$ element suggests that the HCF-1$_{SAS2N}$ element does not precisely colocalize with the region that promotes cell proliferation in tsBN67 cells, and thus one or more additional functions of the basic region, such as possibly association with GABP (25), are required to rescue the tsBN67 defect.

Fine mapping of the paired HCF-1$_{SAS1N}$ and HCF-1$_{SAS1C}$ elements. To map one pair of SAS elements in detail, we performed a deletion analysis of the HCF-1$_{SAS1N}$ and HCF-1$_{SAS1C}$ elements as shown in Fig. 5A. The results of the anal-
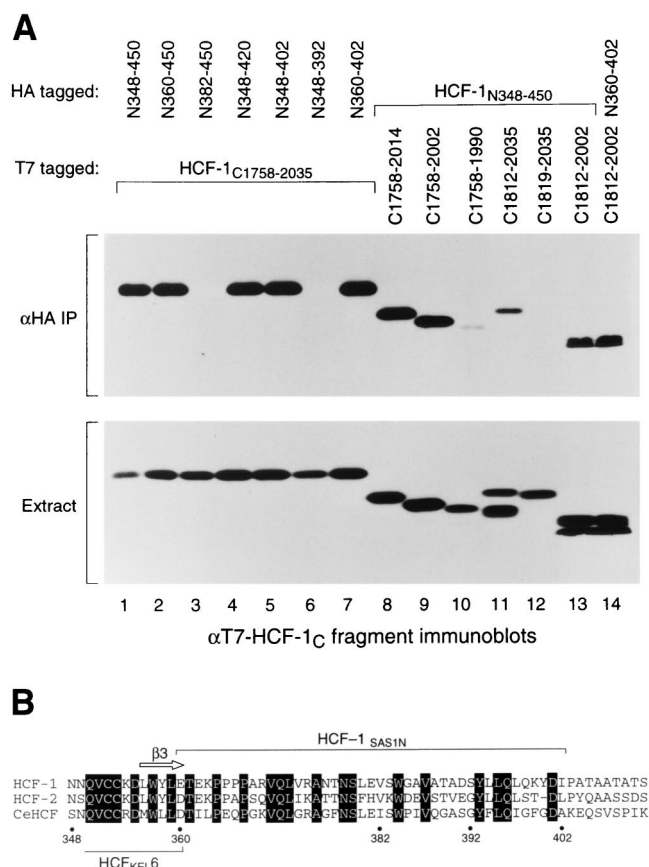
A

B

FIG. 5. Fine mapping of the HCF-1$_{SAS1N}$ and HCF-1$_{SAS1C}$ regions. (A) HA-tagged HCF-1$_N$ fragments (fused to GAL4 residues 1 to 94) and T7-tagged HCF-1$_C$ fragments were coexpressed in transfected 293T cells, and noncovalent association was assayed by immunoprecipitation (IP) with the αHA antibody followed by immunoblotting with the αT7 antibody. Truncations of the HA-tagged HCF-1$_{SAS1N}$ domain were assayed by cotransfection with pCGTHCF-1$_{SAS1C}$ (residues 1758 to 2035) and were as follows: HCF-1$_{N348-450}$ (lane 1), HCF-1$_{N360-450}$ (lane 2), HCF-1$_{N382-450}$ (lane 3), HCF-1$_{N348-420}$ (lane 4), HCF-1$_{N348-402}$ (lane 5), HCF-1$_{N348-392}$ (lane 6), and HCF-1$_{N360-402}$ (lane 7). Truncations of T7-tagged HCF-1$_{SAS1C}$ domain were assayed by cotransfection with the HA-tagged HCF-1$_{SAS1N}$ fragment (residues 348 to 450, pCGNGalHCF-1$_{N348-450}$) and were as follows: HCF-1$_{C1758-2014}$ (lane 8), HCF-1$_{C1758-2002}$ (lane 9), HCF-1$_{C1758-1990}$ (lane 10), HCF-1$_{C1812-2035}$ (lane 11), HCF-1$_{C1819-2035}$ (lane 12), and HCF-1$_{C1812-2002}$ (lane 8). The two smallest functional fragments HCF-1$_{N360-402}$ and HCF-1$_{C1812-2002}$ were combined in lane 13. (B) Alignment of the carboxy-terminal end of the HCF-1$_{KEL6}$ and HCF$_{SAS1N}$ sequences with the corresponding regions of HCF-2 (11) and CeHCF (16). Identical residues in all three sequences are highlighted in black. The conservation extends beyond the last β strand (β3) of HCF-1$_{KEL6}$, across the length of the HCF-1$_{SAS1N}$ domain. Amino acid numbers below the sequence refer to HCF-1.

ysis shown in Fig. 4 located the HCF-1$_{SAS1N}$ element to within the 103-amino-acid HCF-1$_{N348-450}$ fragment. This region contains the carboxy-terminal residues of the HCF-1$_{KEL}6$ repeat (residues 348 to 360), which are conserved among the HCF-1, HCF-2, and CeHCF proteins (11, 16), and an additional region conserved among these three proteins (residues 361 to 396) as shown in Fig. 5B. To locate the HCF-1$_{SAS1N}$ element within residues 348 to 450, we performed a more extensive deletion analysis of this region fused to the GAL4 DNA-binding domain. As shown in Fig. 5A (lanes 1 to 3), deletion of residues 348 to 360, but not to 382, had no apparent effect on association with the HCF-1$_{SAS1C}$-containing HCF-1$_{C1758-2035}$ fragment. Also, deletion of residues 450 to 402, but not to 392, had no apparent effect on association with the HCF-1$_{C1758-2035}$ fragment (lanes 4 to 6), suggesting that the 43-amino-acid

segment from 360 to 402 is sufficient to associate with the HCF-1$_{SAS1C}$ element. Indeed, the 360–402 sequence fused to the GAL4 DNA-binding domain is sufficient to associate with the HCF-1$_{C1758-2035}$ fragment (lane 7). Thus, the SAS1N element resides within residues 360 to 402. Interestingly, this region, which lies immediately adjacent to the HCF-1$_{KEL}6$ region, coincides with the 361–401 segment that is conserved among HCF-1, HCF-2, and CeHCF (Fig. 5B).

We performed a similar analysis of the HCF-1$_{SAS1C}$ element (Fig. 5, lanes 8 to 13). Deletion of carboxy-terminal residues 2035 to 2002, but not to 1990, had no apparent effect on association with HCF-1$_{N348-450}$ (lanes 8 to 10), and deletion of residues 1758 to 1812, but not to 1819, had only a small deleterious effect on association with HCF-1$_{N348-450}$ (lanes 11 and 12). (Note that the HCF-1$_{SAS1C1812-2035}$ construct [lane 11] consistently produced a faster-migrating fragment that did not associate with HCF-1$_{N348-450}$; we do not know the origin of this fragment.) Consistent with these results, an HCF-1$_{C1812-2002}$ fragment can associate with the HCF-1$_{N348-450}$ fragment (lane 13). Indeed, the two smallest fragments capable of HCF self-association—the 43-amino-acid HCF-1$_{N360-402}$ fragment and the 191-amino-acid HCF-1$_{C1812-2002}$ fragment—associate with one another (lane 14). Interestingly, the HCF-1$_{SAS1C}$ element lies precisely within the predicted HCF$_{Fn3}$-repeat-containing carboxy-terminal region that is shared among the HCF-1, HCF-2, and CeHCF proteins (residues 1812 to 2002 [Fig. 1B]). The close match between the mapping results and the boundaries of the proposed Fn3 repeats strengthens the prediction that the HCF-1 carboxyl terminus is composed of a conserved pair of Fn3 repeats, which together form the HCF-1$_{SAS1C}$ element.

Hughes et al. (10) have reported a mapping analysis of the HCF-1$_{SAS1}$ element using proteins synthesized in vitro and an assay involving retardation of the mobility of the VP16-induced complex during polyacrylamide gel electrophoresis. Their analysis mapped the HCF-1$_{SAS1N}$ element to within residues 1 to 450 and the HCF-1$_{SAS1C}$ to within residues 1786 to 2035, consistent with the in vivo association assay described here.

HCF-2 contains a conserved SAS1N element. Unlike the HCF-1 protein, HCF-2 and CeHCF do not contain any HCF-1$_{PRO}$ processing repeats and there is no evidence that HCF-2 and CeHCF are proteolytically processed (11) (Y. Liu and W. Herr, unpublished results). Thus, there is no a priori reason to expect the SAS elements of HCF-1 to be conserved in HCF-2 and CeHCF. We were surprised, therefore, to find that the sequences of both the small SAS1N (residues 360 to 402) and larger SAS1C (residues 1812 to 2002) elements are conserved in the HCF-2 and CeHCF proteins (Fig. 1B and 5B). The sequence conservation led us to ask whether HCF-2 contains a functional SAS1 element. Unfortunately, the carboxy-terminal HCF-2 segment corresponding to HCF-1$_{SAS1C}$ could not be synthesized effectively in transfected cells. We therefore tested the ability of the putative amino-terminal SAS1 element (HCF-2 residues 341 to 394) to associate with the HCF-1$_{SAS1C}$ region as shown in Fig. 6. Consistent with an HCF-2$_{SAS1N}$ function, this HCF-2$_{341-394}$ segment could associate effectively with HCF-1$_{SAS1C}$ (compare lanes 1 to 3). Thus, HCF-2 and perhaps CeHCF are likely to possess HCF self-association activity.

Association with the carboxy-terminal HCF-1$_C$ subunit results in nuclear localization of the HCF-1$_N$ subunit. Immunofluorescence and subcellular fractionation studies have shown that HCF-1 is predominantly a nuclear protein (12–14, 29) and that nuclear localization is determined by a consensus bipartite NLS (5) at its carboxyl terminus (**KRPMSSPEMKSAPKKSK**;
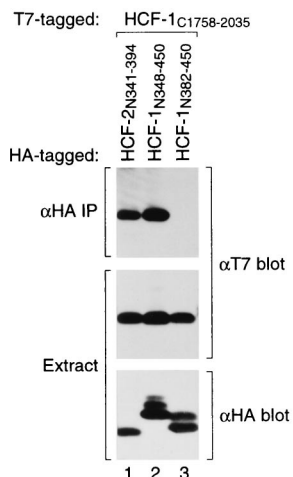
FIG. 6. HCF$_{SAS1}$ function is conserved between HCF-1 and HCF-2. T7-tagged HCF-1$_{C1758–2035}$ was coexpressed in transfected 293T cells with HA-tagged fragments (fused to GAL4 residues 1 to 94) corresponding to residues 341 to 394 of HCF-2 (lane 1), 348 to 450 of HCF-1 (lane 2), and 382 to 450 of HCF-1 (lane 3). HCF-1$_{SAS1N}$ and HCF-1$_{SAS1C}$ association was assayed by coimmunoprecipitation (IP) with the αHA antibody followed by immunoblotting with the αT7 antibody (upper panel). Protein expression was confirmed by immunoblotting extracts directly with the αT7 (center panel; HCF-1$_C$ polypeptides) or αHA (lower panel; HCF-1$_C$ polypeptides) antibody.

residues 2015 to 2031) (14). Thus, when expressed separately, the HCF-1$_{C600}$ fragment accumulates in the nucleus (Fig. 7B) like the endogenous protein (Fig. 7F), and the HCF-1$_{N1011}$ fragment accumulates largely in the cytoplasm (Fig. 7A). De-

letion of the NLS sequence results in HCF-1$_C$ remaining largely in the cytoplasm (Fig. 7B and C).

The dependence of HCF-1 nuclear localization on a single sequence at its carboxyl terminus suggests that following proteolytic processing of the precursor, HCF-1 self-association maintains the HCF-1$_N$ subunit within the nucleus. To test this hypothesis, we asked whether, when synthesized separately in the same cell, the HCF-1$_C$ subunit can affect the subcellular localization of the HCF-1$_N$ subunit. Indeed, synthesis of the wild-type HCF-1$_{C600}$ subunit (Fig. 7D), but not the HCF-1$_{C600\Delta NLS}$ subunit (Fig. 7E), resulted in nuclear import of the HCF-1$_N$ subunit. These results show that the HCF-1$_C$ subunit can recruit the HCF-1$_N$ subunit to the nucleus. Such an activity of HCF-1 subunits could be important for the nuclear retention of the HCF-1$_N$ subunit after nuclear breakdown and resynthesis as a result of mitosis.

DISCUSSION

We have characterized the sequences required for HCF-1$_N$ and HCF-1$_C$ subunit association. To our surprise, this characterization revealed two matched pairs of HCF-1$_N$ and HCF-1$_C$ SAS elements: HCF-1$_{SAS1}$, consisting of HCF-1$_{SAS1N}$ and HCF-1$_{SAS1C}$ partners, and HCF-1$_{SAS2}$, consisting of HCF-1$_{SAS2N}$ and HCF-1$_{SAS2C}$ partners. The positions of the two sets of HCF-1 SAS elements are shown in Fig. 8A. The HCF-1$_{SAS1}$ pair of elements has been mapped with considerable precision and represents a small 43-amino-acid amino-terminal HCF-1$_{SAS1N}$ sequence (residues 360 to 402) immediately adjacent to the β-propeller-containing VP16 interaction domain and a
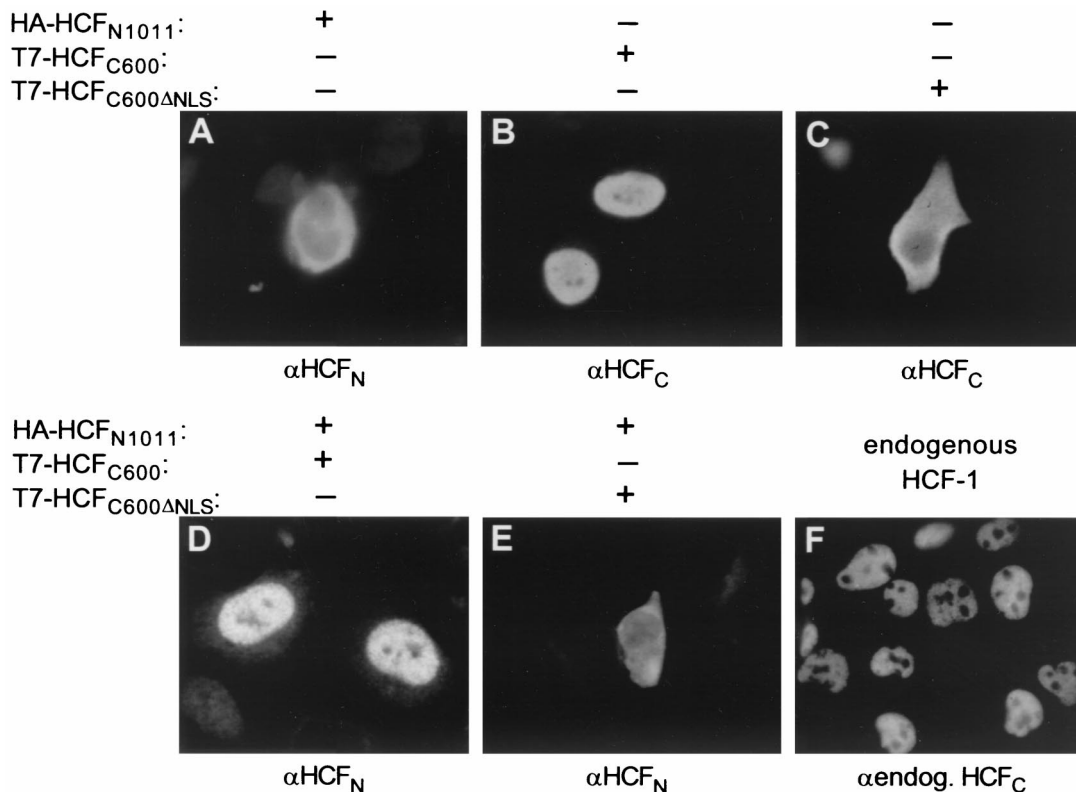

FIG. 7. Nuclear localization of the HCF-1$_N$ subunit through association with the HCF-1$_C$ subunit, visualized by Immunofluorescence of transfected 293 cells using the αHA (A, D, and E) or αT7 (B and C) primary antibody. Cells were transfected with plasmids pCGNHCF-1$_N$ (A), pCGTHCF-1$_C$ (B), pCGTHCF-1$_{C\Delta NLS}$ (C), pCGNHCF-1$_{N1011}$ and pCGTHCF-1$_C$ (D), and pCGNHCF-1$_{N1011}$ and pCGTHCF-1$_{C\Delta NLS}$ (E). For comparison, mock-transfected cells were probed with αHCF-M2 (αendog. HCF$_C$ [F]), a monoclonal antibody against HCF-1 (28).
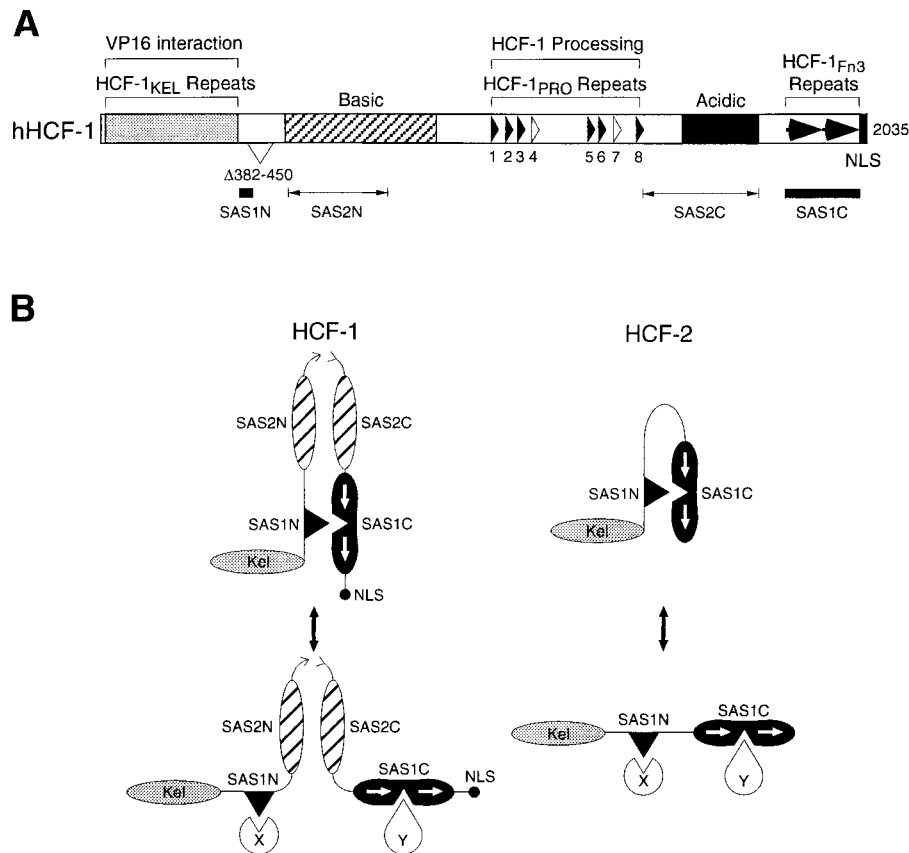
FIG. 8. Summary of HCF-1 functional elements and model for HCF-1 and HCF-2 self-association and association with putative effector proteins. (A) Schematic of human HCF-1 (hHCF-1) showing the locations of the two matched pairs of SAS elements (SAS1 and SAS2). The HCF-1$_{SAS1}$ pair have been mapped to residues 360 to 402 (SAS1N) and 1812 to 2002 (SAS1C). The HCF-1$_{SAS2}$ pair are less well defined and lie between residues 491 and 755 (SAS2N) and residues 1436 and 1756 (SAS2C). Features of the HCF-1 illustration are as described in the legend to Fig. 1A. (B) Self-association is likely to be regulated in vivo. The proposed general structure of HCF-1 is shown in cartoon form. Following proteolytic cleavage at the central HCF$_{PRO}$ repeats, the HCF-1$_N$ and HCF-1$_C$ subunits remain associated through noncovalent interactions mediated by the two self-association domains present in each subunit. Subunit interaction is required for the nuclear localization of HCF-1$_N$, which does not contain its own NLS. The presence of two intersubunit contacts also allows for limited dissociation. For example, following dissociation of the SAS1 pairing, contacts between the two HCF-1 subunits may be maintained by the SAS2 interaction. In this scenario, the SAS1 sequences are available for interaction with other cellular proteins (X and Y), a dual function that might explain the strong sequence conservation of the SAS1 sequences in HCF-2 and CeHCF. Because HCF-2 is not proteolytically cleaved, there is no requirement for a second noncovalent SAS2-like association.

larger 191-amino-acid carboxy-terminal HCF-1$_{SAS1C}$ sequence (residues 1812 to 2002), which contains a pair of Fn3-type repeats. The HCF-1$_{SAS2}$ element has been less rigorously mapped: the HCF-1$_{SAS2N}$ sequence lies within residues 491 to 755 in the so-called, basic region and the HCF-1$_{SAS2C}$ sequence lies within residues 1436 to 1756, which contains the so-called acidic region.

Regulation of HCF-1$_N$ and HCF-1$_C$ association. The identification of two separate SAS elements raises a paradox because deletion of just one half of one of these sets, HCF-1$_{SAS1N}$, inactivates HCF-1 subunit association. These results suggest that amino-terminal HCF-1 sequences can inhibit the activity of the HCF-1$_{SAS2N}$ element. First, the entire amino-terminal region of HCF-1 (residues 1 to 1011) associates less well with the HCF-1$_{SAS2C}$ region than residues 450 to 1011 alone (Fig. 3); second, deletion of residues 380 to 452 in the alternative-splice HCF-1 variant (Fig. 1), which impinges on the HCF-1$_{SAS1N}$ but not the HCF-1$_{SAS2N}$ sequence, prevents detectable HCF-1$_C$ association. Thus, inactivation of HCF-1$_{SAS1N}$ in this natural deletion variant also functionally inactivates HCF-1$_{SAS2N}$. Perhaps, the region encompassing the HCF-1$_{SAS1N}$ sequence inhibits the activity of the HCF-1$_{SAS2N}$ element, particularly when residues 382 to 450 are removed,

providing an efficient mechanism for regulation of HCF subunit association. Whatever the case, this result shows that HCF-1$_{SAS2}$ element is not simply due to nonspecific association of the basic and acidic regions of HCF.

The HCF-1$_{SAS1}$ association element is conserved in HCF family members. The SAS elements in HCF-1 were identified because HCF-1 is processed to produce amino-terminal and carboxy-terminal HCF subunits that remain associated (27). We were very much surprised, therefore, to find that the sequence of one of the paired HCF-1 SAS elements, HCF-1$_{SAS1}$, is conserved in human HCF-2 and C. elegans HCF (Fig. 1B and 5B), proteins that do not display any evidence of proteolytic cleavage. Furthermore, the sequence in HCF-2 corresponding to the HCF-1$_{SAS1N}$ sequence can associate with the HCF-1$_{SAS1C}$ sequence (Fig. 6). Thus, even though there is no evidence that HCF-1 and HCF-2 associate with one another in vivo (K. M. Johnson and A. C. Wilson, unpublished results), both proteins have conserved HCF$_{SAS1N}$ activity. As illustrated in Fig. 8B, we hypothesize that the HCF$_{SAS1}$ element has been conserved in both proteins and retains self-association activity in HCF-2. Given the sequence conservation in C. elegans HCF, we also suggest that the C. elegans HCF protein possesses an

active HCF-1$_{SAS1}$ element, although this possibility has not been tested directly.

It is curious that HCF-2 (and perhaps *C. elegans* HCF) has conserved a SAS element when there is no evidence that it is proteolytically processed. It is also surprising that the HCF-2$_{SAS1N}$ element has retained the ability to associate with HCF-1 when there is no reason to believe that these proteins associate with one another in vivo. Perhaps, the function of the HCF-1$_{SAS1}$ element is not only to associate with itself but also to associate with effector proteins in the cell (Fig. 8B). If, for example, the HCF-1$_{SAS1N}$ and HCF-2$_{SAS1N}$ elements share effector proteins, then the HCF$_{SAS1N}$ element may have been conserved in both HCF-1 and HCF-2 to maintain this interaction, a by-product being the conserved ability of the HCF-2$_{SAS1N}$ element to associate with the HCF-1$_{SAS1C}$ element.

We do not know why HCF-2 may have conserved an SAS element. Its conservation in HCF-2, however, helps explain why HCF-1 unexpectedly has two SAS elements: the first, SAS1, may play a role in both HCF-1 and HCF-2 in addition to self-association. Because, HCF-1, unlike HCF-2, is proteolytically cleaved, the SAS2 element may be essential in HCF-1 to maintain self-association, an activity not required in HCF-2 because it is not proteolytically cleaved.

Fn3 repeats form a protein-protein interaction module. The sequence of the HCF-1$_{SAS1C}$ element exhibits similarity to a tandem pair of Fn3 repeats. Fn3 repeats from different proteins generally exhibit limited sequence similarity (2). Structurally, however, all Fn3 repeats fold into two β sheets packed against each other like a sandwich (3, 4, 9, 18). Thus, Fn3 repeats represent a conserved structure that can vary considerably in sequence to create many different types of functional surfaces. This flexibility may account for their widespread use (2).

Fn3 repeats mediate protein-protein interactions. In some instances, a single repeat is sufficient (20); in other instances, multiple repeats are required for specific association (21). In HCF-1$_{SAS1C}$, both repeats are necessary for association with HCF-1$_{SAS1N}$ (Fig. 5). Recently, de Pereda et al. (3) described the structure of tandem Fn3 repeats from the cytoplasmic tail of the β$_4$ subunit of integrin α$_6$β$_4$. This and other Fn3 repeat structures suggest two ways in which tandem Fn3 repeats can associate with other proteins. In one way, an Fn3 repeat can present short peptide sequences on its surface that can bind other proteins as in the case of the RGD tripeptide sequence of the 10th Fn3 repeat of fibronectin (3). In the second way, tandem Fn3 repeats can form an extended groove that is an attractive docking site for another protein surface. If the HCF-1$_{SAS1C}$ Fn3 repeats form such a surface, it could be a docking site for the HCF-1$_{SAS1N}$ element and perhaps an effector protein as illustrated in Fig. 8B.

Implications of the two-subunit composition of HCF-1 for its function. Consistent with earlier results (14), we have identified a classical bipartite NLS at the extreme carboxyl terminus of HCF-1. We have also shown that the HCF-1$_N$ subunit does not contain an NLS and that HCF-1$_{SAS1N}$ subunits can migrate to the nucleus through association with the HCF-1$_{SAS1C}$ subunit. This arrangement resembles polymerase α primase, which is also composed of two stably associated subunits. In this case, a single NLS in the p54 subunit targets the smaller p46 subunit to the nucleus (19). Pulse-chase analysis of the HCF-1$_{300}$ precursor has shown that it migrates to the nucleus prior to its initial proteolytic cleavage (29). Thus, HCF-1 subunit association is more likely to be required for the nuclear retention of the HCF-1$_N$ subunit rather than its initial nuclear import. Because HCF-1 is stable (29), it may persist through multiple rounds of cell division. Perhaps HCF-1 subunit association is required to maintain the nuclear location of the HCF-1$_N$ subunit following nuclear breakdown and resynthesis as a result of mitosis.

The HCF-1$_N$ and HCF-1$_C$ subunits perform different functions within the cell. The HCF-1$_N$ subunit associates with the viral and cellular HCF-binding proteins VP16 (15, 26), LZIP (6, 17), and GABP (25) and complements the temperature-sensitive cell proliferation defect in tsBN67 cells. As shown here, the HCF-1$_C$ subunit localizes the HCF-1 protein in the nucleus, and it can also stabilize VP16-induced complex formation with full-length VP16 (15). The regulated association of HCF-1 subunits, as evidenced by the alternative pre-mRNA splice variant, provides a unique opportunity to control the association of the different HCF-1$_N$ and HCF-1$_C$ subunit functions in the cell. It will be interesting to determine whether HCF-1$_N$ and HCF-1$_C$ subunit association is temporally regulated during phases of the cell cycle or in specific cell types.

REFERENCES

1. **Altschul, S. F., W. Gish, W. Miller, E. W. Myers, and D. J. Lipman.** 1990. Basic local alignment search tool. J. Mol. Biol. **215:**403–410.
2. **Campbell, I. D., and C. Spitzfaden.** 1994. Building proteins with fibronectin type III modules. Structure **2:**333–337.
3. **de Pereda, J. M., G. Wiche, and R. C. Liddington.** 1999. Crystal structure of a tandem pair of fibronectin type III domains from the cytoplasmic tail of integrin alpha6beta4. EMBO J. **18:**4087–4095.
4. **Dickinson, C. D., B. Veerapandian, X. P. Dai, R. C. Hamlin, N. H. Xuong, E. Ruoslahti, and K. R. Ely.** 1994. Crystal structure of the tenth type III cell adhesion module of human fibronectin. J. Mol. Biol. **236:**1079–1092.
5. **Dingwall, C., and R. A. Laskey.** 1991. Nuclear targeting sequences—a consensus? Trends Biochem. Sci. **16:**478–481.
6. **Freiman, R. N., and W. Herr.** 1997. Viral mimicry: common mode of association with HCF by VP16 and the cellular protein LZIP. Genes Dev. **11:**3122–3127.
7. **Goto, H., S. Motomura, A. C. Wilson, R. N. Freiman, Y. Nakabeppu, K. Fukushima, M. Fujishima, W. Herr, and T. Nishimoto.** 1997. A single-point mutation in HCF causes temperature-sensitive cell-cycle arrest and disrupts VP16 function. Genes Dev. **11:**726–737.
8. **Herr, W.** 1998. The herpes simplex virus VP16-induced complex: mechanisms of combinatorial transcriptional regulation. Cold Spring Harbor Symp. Quant. Biol. **63:**599–607.
9. **Huber, A. H., Y. M. Wang, A. J. Bieber, and P. J. Bjorkman.** 1994. Crystal structure of tandem type III fibronectin domains from Drosophila neuroglian at 2.0 Å. Neuron **12:**717–731.
10. **Hughes, T. A., S. LaBoissière, and P. O'Hare.** 1999. Analysis of functional domains of the host cell factor involved in VP16 complex formation. J. Biol. Chem. **274:**16437–16443.
11. **Johnson, K. M., S. S. Mahajan, and A. C. Wilson.** 1999. Herpes simplex virus transactivator VP16 discriminates between HCF-1 and a novel family member, HCF-2. J. Virol. **73:**3930–3940.
12. **Kristie, T. M., J. L. Pomerantz, T. C. Twomey, S. A. Parent, and P. Sharp, A.** 1995. The cellular C1 factor of the herpes simplex virus enhancer complex is a family of polypeptides. J. Biol. Chem. **270:**4387–4394.
13. **Kristie, T. M., J. L. Vogel, and A. E. Sears.** 1999. Nuclear localization of the C1 factor (host cell factor) in sensory neurons correlates with reactivation of herpes simplex virus from latency. Proc. Natl. Acad. Sci. USA **96:**1229–1233.
14. **LaBoissière, S., T. Hughes, and P. O'Hare.** 1999. HCF-dependent nuclear import of VP16. EMBO J. **18:**480–489.
15. **LaBoissière, S., S. Walker, and P. O'Hare.** 1997. Concerted activity of host cell factor subregions in promoting stable VP16 complex assembly and preventing interference by the acidic activation domain. Mol. Cell. Biol. **17:**7108–7118.
16. **Liu, Y., M. O. Hengartner, and W. Herr.** 1999. Selected elements of herpes simplex virus accessory factor HCF are highly conserved in *Caenorhabditis elegans.* Mol. Cell. Biol. **19:**909–915.
17. **Lu, R., P. Yang, P. O'Hare, and V. Misra.** 1997. Luman, a new member of the

CREB/ATF family, binds to herpes simplex virus VP16-associated host cell factor. Mol. Cell. Biol. **17:**5117–5126.

18. **Main, A. L., T. S. Harvey, M. Baron, J. Boyd, and I. D. Campbell.** 1992. The three-dimensional structure of the tenth type III module of fibronectin: an insight into RGD-mediated interactions. Cell **71:**671–678.

19. **Mizuno, T., T. Okamoto, M. Yokoi, M. Izumi, A. Kobayashi, T. Hachiya, K. Tamai, T. Inoue, and F. Hanaoka.** 1996. Identification of the nuclear localization signal of mouse DNA primase: nuclear transport of p46 subunit is facilitated by interaction with p54 subunit. J. Cell Sci. **109:**2627–2636.

20. **Moyano, J. V., B. Carnemolla, C. Dominguez-Jimenez, M. Garcia-Gila, J. P. Albar, P. Sanchez-Aparicio, A. Leprini, G. Querze, L. Zardi, and A. Garcia-Pardo.** 1997. Fibronectin type III5 repeat contains a novel cell adhesion sequence, KLDAPT, which binds activated alpha4beta1 and alpha4beta7 integrins. J. Biol. Chem. **272:**24832–24836.

21. **Nagai, T., N. Yamakawa, S. Aota, S. S. Yamada, S. K. Akiyama, K. Olden, and K. M. Yamada.** 1991. Monoclonal antibody characterization of two distant sites required for function of the central cell-binding domain of fibronectin in cell adhesion, cell migration, and matrix assembly. J. Cell. Biol. **114:**1295–1305.

22. **O'Hare, P.** 1993. The virion transactivator of herpes simplex virus. Semin. Virol. **4:**145–155.

23. **Schultz, J., F. Milpetz, P. Bork, and C. P. Ponting.** 1998. SMART, a simple modular architecture research tool: identification of signaling domains. Proc. Natl. Acad. Sci. USA **95:**5857–5864.

24. **Sturm, R. A., G. Das, and W. Herr.** 1988. The ubiquitous octamer-binding protein Oct-1 contains a POU domain with a homeo box subdomain. Genes Dev. **2:**1582–1599.

25. **Vogel, J. L., and T. M. Kristie.** 2000. The novel coactivator C1 (HCF) coordinates multiprotein enhancer formation and mediates transcription activation by GABP. EMBO J. **19:**683–690.

26. **Wilson, A. C., R. N. Freiman, H. Goto, T. Nishimoto, and W. Herr.** 1997. VP16 targets an amino-terminal domain of HCF involved in cell-cycle progression. Mol. Cell. Biol. **17:**6139–6146.

27. **Wilson, A. C., K. LaMarco, M. G. Peterson, and W. Herr.** 1993. The VP16 accessory protein HCF is a family of polypeptides processed from a large precursor protein. Cell **74:**115–125.

28. **Wilson, A. C., J. E. Parrish, H. F. Massa, D. L. Nelson, B. J. Trask, and W. Herr.** 1995. The gene encoding the VP16-accessory protein HCF (HCFC1) resides in human Xq28 and is highly expressed in fetal tissues and the adult kidney. Genomics **25:**462–468.

29. **Wilson, A. C., M. G. Peterson, and W. Herr.** 1995. The HCF repeat is an unusual proteolytic cleavage signal. Genes Dev. **9:**2445–2458.